

Chlorophyll nitrogen isotope values track shifts between cyanobacteria and eukaryotic algae in a natural phytoplankton community in Lake Erie

Jenan J. Kharbush^{*a}, Derek J. Smith^b, McKenzie Powers^b, Henry A. Vanderploeg^c, David Fanslow^c, Rebecca S. Robinson^d, Gregory J. Dick^b, Ann Pearson^a

^a*Department of Earth and Planetary Sciences, Harvard University, 20 Oxford St., Cambridge, MA 02138, USA*

^b*Department of Earth and Environmental Sciences, University of Michigan, 1100 North University Ave., Ann Arbor, Michigan 48109, USA*

^c*NOAA–GLERL, 4840 S. State Rd., Ann Arbor, Michigan 48108, USA*

^d*Graduate School of Oceanography, University of Rhode Island, 215 S Ferry Rd, Narragansett, RI 02882, USA*

* Corresponding author. Tel.: (608) 843-8517. Primary email address:

jkharbush@fas.harvard.edu Alternate email address: jenanj@gmail.com

2 **ABSTRACT**

3 Chlorophylls are produced by all photosynthetic organisms and are ideal targets for compound-
4 specific isotopic studies of phytoplankton. In laboratory cultures, the difference between the
5 nitrogen (N) isotope ratio ($\delta^{15}\text{N}$ value) of chlorophyll and the $\delta^{15}\text{N}$ value of biomass, known as
6 ϵ_{por} , varies taxonomically, yielding potential applications for studying productivity in modern
7 and ancient environments. Here we take advantage of the annual cyanobacterial bloom in Lake
8 Erie, USA, to demonstrate ϵ_{por} patterns in a natural community. The resulting time series shows
9 that environmental observations are similar to laboratory cultures: predicted ϵ_{por} endmember
10 values range from 4.6‰ to 7.4‰ for eukaryotic algae, and -18‰ to -21‰ for cyanobacteria.
11 Because the range and sensitivity of ϵ_{por} is similar between laboratory and natural settings, the
12 data support the use of ϵ_{por} as a reliable tracer of the relative contributions of cyanobacteria and
13 eukaryotic algae to nutrient utilization and primary production in lacustrine environments.

14

15 *Keywords:* Isotope ratios; cyanobacteria; Lake Erie; biomarkers; primary production

16

17 **1. Introduction**

18 Along with phosphorus (P), nitrogen (N) is a major limiting nutrient for primary
19 production in aquatic ecosystems, where N cycling is largely driven by microbial
20 transformations that convert N between its oxidized and reduced forms. Each of these
21 transformations, including N-fixation, nitrification and denitrification, has an associated kinetic
22 isotope effect that describes the ^{15}N content of the product relative to the substrate in the reaction
23 (summarized in Sigman et al., 2009). N isotope ratios ($\delta^{15}\text{N}$ values) of phytoplankton biomass in
24 surface waters therefore record an integrated signal of the sources and forms of N used for algal

25 growth. $\delta^{15}\text{N}$ values of bulk organic matter can be preserved long-term in the geological record
26 and serve as a tracer for variations in redox state (Jenkyns et al., 2001; Godfrey and Falkowski,
27 2009), major modes of primary production (Calvert et al., 1992; Struck et al., 2000), and nutrient
28 source availability in the euphotic zone (Hodell and Schelske, 1998; Teranes and Bernasconi,
29 2000). However, diagenesis both before and after burial can alter the bulk N pool that is
30 ultimately preserved, complicating interpretations of sedimentary isotope data (Sigman et al.,
31 1999; Robinson et al., 2004, 2012; Tesdal et al., 2013).

32 To complement bulk analyses, an additional approach is to use compound-specific $\delta^{15}\text{N}$
33 analysis of organic molecules that are not affected by diagenesis (Chicarelli et al., 1993; Sachs et
34 al., 1999; Chikaraishi et al., 2008; Higgins et al., 2009; Ren et al., 2009). Chlorophylls are
35 frequent biomarker targets because they are an essential part of the photosynthetic apparatus and
36 are therefore specific for surface water processes. Importantly, the N bonds in chlorophylls are
37 not altered by diagenesis (Louda and Baker, 1986), and therefore the diagenetic products of
38 chlorophylls retain the original isotopic signature (Tyler et al., 2010). Even accounting for the
39 minor isotope effect likely associated with the formation of metalloporphyrins in sediments
40 (Junium et al., 2015), compound-specific $\delta^{15}\text{N}$ measurement of chlorophylls and their
41 degradation products are a more direct tracer of N utilization by phytoplankton than $\delta^{15}\text{N}$ values
42 of bulk organic matter alone.

43 For chlorophyll $\delta^{15}\text{N}$ values to be useful, however, the isotopic relationship between
44 chlorophyll and total biomass must be well understood. Several previous studies have examined
45 patterns of biosynthetic N isotope fractionation in cultured organisms (Sachs et al., 1999;
46 Beaumont et al., 2000; Higgins et al., 2011; Tsao et al., 2012). This parameter, defined as ϵ_{por} ,
47 represents the isotopic offset between cellular biomass and chloropigment: $\epsilon_{\text{por}} \approx \delta^{15}\text{N}_{\text{biomass}} -$

48 $\delta^{15}\text{N}_{\text{chloropigment}}$. This definition follows the convention that positive values of ϵ correspond to
49 depletion of the heavy isotope relative to the starting material (Hayes, 2001).

50 ϵ_{por} appears to be taxonomically diagnostic for three main algal groups (Fig. 1). The
51 eukaryotic algae have a median ϵ_{por} value of $5.5 \pm 1.6\%$, indicating that they biosynthesize
52 chlorophyll that is $\sim 5.5\%$ depleted in ^{15}N relative to cellular biomass. Marine cyanobacteria
53 have a median ϵ_{por} value of $0.2 \pm 2.5\%$, showing on average no fractionation between biomass
54 and chlorophyll. Finally, the freshwater cyanobacteria have a median ϵ_{por} value of $-10.3 \pm 2.6\%$,
55 meaning the chlorophyll is enriched, or isotopically “heavy”, relative to biomass. The ϵ_{por}
56 signature of freshwater cyanobacteria is especially striking, given that biosynthetic reactions
57 usually yield products that are isotopically depleted relative to reactants (Hayes, 2001).

58 These patterns in ϵ_{por} hold true across a wide range of culture experiments, regardless of
59 the N substrate and its isotopic composition (NO_3^- , NH_4^+ , or N_2 -fixing; Higgins et al., 2011) or
60 whether grown in batch or chemostat culture (Tsao et al., 2012). In other words, while N-
61 assimilating enzymes do fractionate each N substrate differently and therefore affect the whole
62 cell $\delta^{15}\text{N}$ value, the isotopic offset between chlorophylls and cellular biomass remains the same
63 within each algal group. This independence from the type(s) of N substrate, combined with the
64 significant differences between the eukaryotic and cyanobacterial endmembers for ϵ_{por} , makes
65 ϵ_{por} a useful tool for reconstructing phytoplankton export production in modern and ancient
66 marine environments (Higgins et al., 2012; Shen et al., 2018). However, to date the use of ϵ_{por}
67 has been limited, because the physiological and/or biochemical basis for the observed taxonomic
68 differences remains unknown. In addition, the patterns in ϵ_{por} are primarily a conclusion of
69 laboratory culture studies.

70 Environmental evidence for these patterns remains limited. An early study reported two
71 measurements of ϵ_{por} from a cyanobacteria-dominated freshwater lake in Japan (Katase and
72 Wada, 1990), where the ϵ_{por} values of approximately -13‰ and -16‰ can now be interpreted as
73 consistent with ϵ_{por} values for freshwater cyanobacterial cultures. However, recent studies have
74 documented a marine intertidal cyanobacterial (*Lyngbya* sp.) mat with an ϵ_{por} value of -10.1‰
75 (Fulton et al., 2012, close to the freshwater cyanobacterial endmember), and a freshwater
76 meromictic lake dominated by *Synechococcus* sp. with an ϵ_{por} value of -0.4‰ (close to the
77 marine cyanobacterial endmember; Fulton et al., 2018). These results suggest that patterns of ϵ_{por}
78 may be more variable in natural systems than in culture, and that exploration of additional
79 environmental settings is needed.

80 To further establish the environmental expression of ϵ_{por} , we sought a system with clearly
81 distinguishable phytoplankton community endmembers. Lake Erie is an ideal location, because it
82 experiences an annual shift in the phytoplankton community from eukaryotic phytoplankton in
83 the early summer to cyanobacteria in the late summer/early fall (Bridgeman et al., 2012). Lake
84 Erie is the shallowest and most productive of the Laurentian Great Lakes and has experienced
85 significant eutrophication over the last half-century. Despite initial improvements achieved by
86 the reduction of total P inputs to the lake via the Great Lakes Water Quality Agreement, the lake
87 has become eutrophic since the mid-1990s, as evidenced by increased water column hypoxia
88 (Zhou et al., 2013; Del Giudice et al., 2018) and by large annual cyanobacterial harmful algal
89 blooms (CHABs) dominated by toxin-forming strains of the non-diazotrophic cyanobacteria
90 *Microcystis* sp. (Michalak et al., 2013; Berry et al., 2017). The intensity of these blooms has
91 increased in the last decade (Stumpf et al., 2012), resulting in several blooms that impacted the

92 drinking water supply for the city of Toledo (Michalak et al., 2013; Carmichael and Boyer,
93 2016).

94 In this study, we took advantage of this annual CHAB event in Lake Erie to investigate
95 whether ϵ_{por} values track the transition in the phytoplankton community over the course of the
96 bloom. We hypothesized that ϵ_{por} should shift from positive values (^{15}N -depleted chlorophyll)
97 during pre-bloom, eukaryote-dominated conditions in the early summer to more negative values
98 (^{15}N -enriched chlorophyll) during the height of the CHAB in late summer and into fall.

99

100 **2. Materials and methods**

101 *2.1. Sample collection*

102 Weekly samples were collected from the water column at station WE2 (41°46' N, 83°0'
103 W) in the western basin of Lake Erie, USA (Fig. 2), from June through October 2017, for a total
104 of 18 time points. Twenty liters of depth-integrated water was collected with a peristaltic pump
105 by slowly moving a weighted Tygon tube up and down from the surface of the water column to
106 one meter from lake bottom (0–5 m depth on average). The water was filtered through 0.7 μm
107 GF/F filters (142 mm diameter, Whatman), which were frozen and stored at $-80\text{ }^{\circ}\text{C}$.

108 Approximately 10% of each filter was reserved for bulk $\delta^{15}\text{N}$ analysis, while the remainder was
109 extracted for chlorophyll $\delta^{15}\text{N}$ analysis. If the sample needed to be filtered onto multiple GF/F
110 filters, a fraction for bulk analysis was reserved from each filter to ensure representative
111 sampling. For chlorophyll analysis, these multiple filters were combined for extraction, except in
112 a few cases where they were analyzed separately to verify that variability between filters for a
113 single time point was low. Detailed sample information is available in Supplementary Table S1.

114

115 2.2. *Phytoplankton community composition*

116 Phytoplankton community composition was determined using a submersible FluoroProbe
117 (bbe Moldaenke GmbH, Germany), which monitors in situ chlorophyll fluorescence. The
118 FluoroProbe quantifies four broad ‘spectral groups’ of chlorophyll *a*-containing phytoplankton
119 (expressed in $\mu\text{g Chl}a \text{ L}^{-1}$), based on differences in their accessory light harvesting pigments that
120 result in characteristic fluorescence fingerprints (Beutler et al., 2002; Johnsen and Sakshaug,
121 2007; Escoffier et al., 2015). Phytoplankton groups that can be distinguished are: (i) green algae
122 (ii) cyanobacteria, (iii) diatoms/dinoflagellates/chrysophytes and (iv) cryptophytes. In Lake Erie,
123 group iii is dominated by diatoms, and hereafter will be referred to as the diatom group.
124 Fluorescence profiles of pigment concentration for each group were depth-integrated for the top
125 5 m and normalized to the total chlorophyll concentration to give the fraction of chlorophyll
126 contributed by each group.

127

128 2.3. *Chlorophyll extraction and $\delta^{15}\text{N}$ analysis*

129 Chlorophyll was extracted from GF/Fs in a 2:1 (v/v) mixture of
130 dichloromethane/methanol (DCM/MeOH) with vortexing (1 min) followed by sonication in an
131 immersion bath (10 min) and incubation in the dark at 4 °C for at least 2 h. Filter pieces were
132 removed using centrifugation and filtration, and the extract concentrated under N_2 gas using a
133 Turbovap II (Zymark). Silica gel columns were prepared by adding glass wool, dry Na_2SO_4 , and
134 silica gel to 5" glass pipets, and combusted before use. The concentrated chlorophyll extracts
135 were added to the silica columns and eluted using DCM/MeOH (2:1, v/v).

136 The extracts were further purified for chlorophyll analyses using an HPLC (Agilent 1200
137 series) equipped with multi-wavelength UV/Vis detector. Using a method modified from Higgins

138 et al. (2009), samples were injected onto two ZORBAX SIL columns (4.6×250 mm, $5 \mu\text{m}$)
139 connected in series and eluted at 1 mL min^{-1} using the gradient described in Supplementary
140 Table S2. Chlorophylls were identified using absorbance spectra and comparison to an authentic
141 chlorophyll *a* standard (Sigma-Aldrich), and collected using time-based fraction collection from
142 13 to 17 minutes. Representative HPLC chromatograms are shown in Supplementary Fig. S1.
143 Purified chlorophyll fractions were dried under N_2 gas and reconstituted in DCM.

144 Chlorophyll $\delta^{15}\text{N}$ values were analyzed according to the methods in Higgins et al. (2009).
145 Briefly, chlorophyll was oxidized in DCM in quartz tubes under UV light in a biosafety cabinet
146 for 6 h, dried, and then oxidized chemically using re-crystallized $0.05 \text{ M K}_2\text{S}_2\text{O}_8$ dissolved in
147 fresh 0.15 M NaOH . Purity of isolated chlorins was assessed by comparing measured oxidized
148 NO_3^- yield and predicted NO_3^- yield. Predicted NO_3^- was calculated by conversion from HPLC
149 peak area using chlorophyll standards (as in Higgins et al., 2009). All samples that were
150 collected and processed as single filters gave linear correspondence (slope 1.0, $R^2 = 0.84$)
151 between measured oxidized NO_3^- yield and predicted NO_3^- yield (Supplementary Fig. S2). Three
152 samples that represent combined GF/F filter extracts fell below the 1:1 line (i.e., low NO_3^-
153 yield), likely due to artifacts from extra sample handling. No samples fell significantly above the
154 line, indicating there was no N contributed by non-UV sensitive sources such as amines.

155 Oxidized NO_3^- concentration was measured using a chemiluminescent NO_x analyzer
156 (Teledyne NO/NO_x Analyzer 200E), and $\delta^{15}\text{N}$ values were measured using the denitrifier
157 method (Sigman et al., 2001), on a Delta V Advantage isotope ratio mass spectrometer with a
158 custom built purge and trap system. Isotopic measurements were standardized to the N_2 reference
159 scale using standard reference materials IAEA N3 and USGS 34. $\delta^{15}\text{N}$ values were corrected for
160 a N blank originating from the HPLC solvent and from the oxidizing reagent, according to

161 Higgins et al. (2009).

162

163 2.4. Bulk $\delta^{15}\text{N}$ analysis

164 Subsamples of GF/F filters for bulk isotopic analysis were placed into tin capsules
165 (Costech) and dried at 50 °C overnight. Dry capsules were folded and crushed, and analyzed on a
166 Thermo Scientific Flash IRMS Elemental Analyzer with EA Isolink, coupled to a Delta V
167 Advantage IRMS through a Conflo IV universal interface. Sample $\delta^{15}\text{N}$ values were calculated
168 using in-house laboratory standards as well as standard reference materials USGS40 and
169 USGS41a.

170

171 3. Results

172 The composition of the phytoplankton community at station WE2 is shown in Fig. 3A.
173 Uncertainty in the classification of each phytoplankton group by Fluoroprobe is estimated as \pm
174 5% based on previous literature (Escoffier et al., 2015). In early July the community is mostly
175 eukaryotic, with cyanobacteria contributing < 20% of the total chloropigments. Over the
176 summer, the relative fraction of cyanobacteria increases, with the exception of a brief period in
177 early September, when the cyanobacteria temporarily decrease to 30% before returning to high
178 abundance. By October, cyanobacteria account for > 70% of the chloropigment fluorescence.

179 Bulk and chlorophyll $\delta^{15}\text{N}$ values for each sampling date are shown in Fig. 3B

180 (Supplementary Table S3 contains the numerical values and calculated uncertainties).

181 Throughout the summer, the bulk biomass $\delta^{15}\text{N}$ values spanned from 4.4‰ to 9.3‰ (average
182 7.1‰ \pm 1.6‰), indicating that the surface water nitrogen sources and total nitrogen budget were
183 relatively isotopically stable. In contrast, chlorophyll $\delta^{15}\text{N}$ values spanned a time-evolving range

184 from -4% to 23% , i.e., a seasonal shift of $> 25\%$. The corresponding values of ϵ_{por} track the
185 change from a eukaryote-dominated to cyanobacteria-dominated community, transitioning from
186 mostly positive values in July to negative values in September and October (Fig. 3C).
187 Specifically, ϵ_{por} is strongly correlated with the percentage of cyanobacteria in the community
188 (Fig. 4), becoming more negative as the contribution from cyanobacteria increases. We used both
189 an ordinary least-squares and an orthogonal least-squares regression to predict the range for
190 eukaryotic and cyanobacterial endmembers for ϵ_{por} . The ordinary regression (using only the
191 uncertainty in $\delta^{15}\text{N}$) predicts that ϵ_{por} equals 4.6% when cyanobacteria are absent and -18.4%
192 when cyanobacteria make up 100% of the community (Fig. 4), while the orthogonal regression
193 incorporates the average uncertainties in both the Fluoroprobe and ϵ_{por} measurements (5% and
194 0.8% , respectively) and predicts respective endmembers of 7.4% and -21.6% . Although
195 sediment resuspension did occur at our sampling site, a comparison of turbidity measurements
196 with both chlorophyll $\delta^{15}\text{N}$ and ϵ_{por} values showed no correlation with either, indicating that
197 sediment resuspension of chlorophyll degradation products had no effect on the observed ϵ_{por}
198 relationship (Supplementary Fig. S3).

199

200 **4. Discussion**

201 The correlation between ϵ_{por} and community composition in Lake Erie supports the
202 hypothesis that ϵ_{por} is robustly linked to higher-level taxonomy. Both the chlorophyll $\delta^{15}\text{N}$ (ϵ_{por})
203 and FluoroProbe data target the pigment pool specifically, rather than algal biomass and/or
204 biovolume. This common focus on the same analyte likely explains why the two types of data
205 exhibit such a strong correlation, both qualitatively (e.g., the simultaneous change in both %
206 cyanobacteria and ϵ_{por} indicated by the brief community excursion in September, Fig. 3), as well

207 as quantitatively (Fig. 4). Good correspondence between ϵ_{por} and the proportion of pigments
208 originating from cyanobacteria vs eukaryotic organisms is to be expected if ϵ_{por} is indeed tied to
209 biosynthetic differences in chlorophyll N-isotope fractionation that vary among major algal
210 groups.

211 Importantly, the ϵ_{por} endmember values predicted by the Lake Erie data are consistent
212 with the values from laboratory cultures, both in range and magnitude (e.g., Sachs et al. 1999;
213 Higgins et al., 2011). They also agree broadly with the one prior field observation (Katase and
214 Wada, 1990). The eukaryotic endmember is defined as the scenario where cyanobacteria are
215 completely absent from the phytoplankton community (y-intercept, Fig. 4). Although not
216 realized in this natural community, as the cyanobacterial population never reaches 0%, the
217 predicted range for the extrapolated eukaryotic ϵ_{por} endmember (4.6–7.4‰) overlaps with the
218 median ϵ_{por} value obtained from eukaryotic cultures grown in the laboratory ($5.5 \pm 1.6\%$, Fig. 1).
219 The predicted range for the extrapolated cyanobacterial ϵ_{por} endmember (–18.4‰ to –21.6‰)
220 also is in the same direction as – although significantly more fractionated than – the literature
221 values for cultured cyanobacteria and the data of Katase and Wada (1990). It is possible that
222 cyanobacteria growing naturally in freshwater systems may exhibit even greater ^{15}N -enrichment
223 of chlorophyll relative to biomass than when grown in lab cultures, although the reasons for this
224 are currently unknown.

225 The general agreement between culture studies and the environment is consistent with the
226 idea that there is a fundamental biosynthetic or physiological explanation for why chlorophyll N
227 isotopes are fractionated differently among major algal groups, independent of culture conditions
228 or the original N source (NO_3^- , NH_4^+ , or N_2 ; Higgins et al., 2011). This property suggests ϵ_{por}
229 should be a reliable tracer that can be used across nearly all biogeochemical conditions or

230 nutrient regimes, because shifts in ϵ_{por} appear to be influenced primarily by the phytoplankton
231 group and not by other site-specific environmental factors such as redox state, temperature, or
232 nutrient supply (e.g., N sources, see Supplementary Fig. S4). Exceptions may be unusual systems
233 with large contributions from anoxygenic phototrophs (e.g., Fayetteville Green Lake, Fulton et
234 al., 2018). Although the reason for the difference in characteristic ϵ_{por} values remains unknown,
235 the biosynthetic pathway for chlorophylls is understood to be the same in both cyanobacteria and
236 eukaryotic plankton (Beale, 1999; Sachs et al., 1999). This implies that the expression of
237 different ϵ_{por} values requires either a different kinetic isotope effect for a critical enzyme or a
238 fundamental shift in the balance of branch points around a biosynthetic intermediate (Hayes,
239 2001). In either case, tetrapyrroles are synthesized from the amino acid glutamate; thus, a better
240 understanding of ϵ_{por} values will require further investigation of the specific cellular fates of this
241 amino acid.

242 Importantly, the dominant cyanobacterial species in Lake Erie, *Microcystis*, do not fix N_2 .
243 In a system where N_2 -fixing cyanobacteria are important, the bulk cellular $\delta^{15}\text{N}$ value would shift
244 to reflect the minimal fractionation that occurs with N_2 fixation. The ϵ_{por} values, however, would
245 shift in parallel, as the isotopic offset between chlorophyll and cellular biomass is constant
246 within these major algal groups. This would also be true for other N cycling processes (e.g.,
247 denitrification) that result in N isotope fractionation in the water column. Therefore ϵ_{por}
248 measurements provide integrated information on both the N sources used by phytoplankton (as
249 reflected by individual bulk and chlorin isotope values) and the dominant phototroph type (as
250 indicated by the ϵ_{por} value), independent from other approaches that sample different timescales
251 such as DNA sequencing. Additionally, results from contemporary studies of ϵ_{por} values in the
252 water column can be linked directly to interpretations of the sedimentary record, providing

253 continuity between these types of data.

254 Because the Lake Erie ϵ_{por} data directly reflect the relative ratio of cyanobacteria to
255 eukaryotic algae in the total community, the results support the application of ϵ_{por} as a proxy for
256 the contribution of these groups to primary production and N cycling in aquatic environments.
257 While we chose Lake Erie as a study site specifically because it had a well-defined
258 phytoplankton community, there are many systems where the community is more complex or
259 difficult to define in terms of major contributors to primary production and nitrogen cycling,
260 where ϵ_{por} could also be a useful tracer. For example, benthic algae in riverbeds are important
261 primary producers but their contribution to riverine food webs is still poorly quantified. Recent
262 work examining the isotopic composition of periphyton in riverbeds noted apparently anomalous
263 enriched chlorophyll $\delta^{15}\text{N}$ values relative to bulk $\delta^{15}\text{N}$ values (Ishikawa et al., 2015), a signature
264 that we can now verify likely indicates the presence of cyanobacteria. ϵ_{por} could also be applied
265 in coastal wetlands and estuaries, which are among the most productive ecosystems on Earth;
266 they contain a variety of primary producers that are important in supporting secondary
267 production, including benthic microalgae, as well as both marine and freshwater phytoplankton
268 species. Coastal ecosystems are also vulnerable to anthropogenic changes in nutrient
269 concentration and stoichiometry, with many experiencing community and food web shifts over
270 the past several decades in which the role of N is likely important, but not well quantified (e.g.,
271 the San Francisco Bay Estuary; Glibert et al., 2011). Alongside existing stable isotope
272 techniques, ϵ_{por} could be used to elucidate the relationship between N dynamics and the
273 evolution of phytoplankton communities in these complex ecosystems.

274 This proxy also has applications in paleoenvironmental studies, and indeed has already
275 been applied to the study of ancient marine sediments as a (paleo)-population tracer (Higgins et

276 al., 2012; Gueneli et al., 2018; Shen et al., 2018). Using ϵ_{por} for population reconstruction
277 requires accounting for some uncertainty in the obtained values for the cyanobacterial
278 contribution. However, even a relatively rough estimate of community composition can allow the
279 use of isotope mixing models to quantitatively reconstruct N cycling (see Higgins et al., 2012 for
280 an example of this in a marine environment). In addition, the larger isotopic separation between
281 the eukaryotic and the freshwater cyanobacterial endmembers could facilitate a more sensitive
282 utilization of ϵ_{por} in freshwater sedimentary records, perhaps yielding more accurate population
283 reconstructions than in marine environments. Importantly, the large range of ϵ_{por} values observed
284 in Lake Erie and the linear relationship between ϵ_{por} values and the fraction of cyanobacteria in
285 the community implies that the cyanobacterial contribution should still be detectable even in
286 lakes where cyanobacteria do not currently form blooms (e.g., Lake Superior).

287 A specific application is the use of ϵ_{por} values from Holocene sediment cores to study the
288 history of cyanobacterial expansion in response to eutrophication and anthropogenic alteration of
289 the N cycle, which is a concern in numerous freshwater lakes around the world. Understanding
290 the relationship between nutrient supply and phytoplankton communities in freshwater
291 environments is critical to understanding the factors that drive phytoplankton community shifts
292 and for water quality management efforts, especially for environments heavily impacted by
293 agriculture and/or the effects of impending climate change. For example, a previous study used
294 bulk ^{13}C and ^{15}N isotope measurements of organic matter in sediment cores to reconstruct
295 historic productivity changes in Lake Ontario due to anthropogenic activities (Hodell and
296 Schelske, 1998). However, the authors were unable to explain whether the observed trends in
297 bulk organic matter $\delta^{15}\text{N}$ values after 1970 were due to anthropogenic changes in N sources,

298 phytoplankton community shifts, or both. Use of ϵ_{por} measurements in this setting could
299 potentially resolve this question.

300 ϵ_{por} could also be used to look further back into the pre-anthropogenic past, where the
301 influences of climate and precipitation patterns on the phytoplankton community in lakes are still
302 not well understood. For example, in Lake Erie, recent work showed the intensity of
303 cyanobacterial blooms to be strongly influenced by spring precipitation events that increase river
304 discharge and therefore nutrient inputs to the lake, a synergistic interaction between agriculture
305 practices and climate change (Michalak et al., 2013). Whether similar relationships existed in the
306 pre-anthropogenic past remains to be explored. The evolution of the phytoplankton community
307 over the last 100–150 years in response to eutrophication is mostly inferred through studies
308 utilizing N isotopes of bulk organic matter and the sedimentary record of diatoms (Allinger and
309 Reavie, 2013; Hobbs et al., 2016).

310 Other paleolimnological proxies such as pigment distributions have also been used to
311 successfully document changes in cyanobacterial abundance in other lakes (Taranu et al., 2015).
312 Because of selective preservation of certain pigment types, however, fossil pigment
313 concentrations in sediments alone may be an unreliable measure of the relative abundance of
314 phytoplankton groups (Leavitt, 1993; Leavitt and Findlay, 1994). In contrast, ϵ_{por} values provide
315 a more reliable, quantitative proxy for the relative importance of cyanobacteria to primary
316 production, organic matter export, and N cycling, which is preserved in the sediment record.

317 Although there are clearly environmental exceptions to the patterns defined in cultures
318 that have yet to be explained, it is possible that an intertidal mat (Fulton et al., 2012) and the
319 chemocline of a meromictic lake (Fulton et al., 2018) represent unique biogeochemical habitats
320 for cyanobacteria, such that biosynthesis of chlorophyll is different from the planktonic

321 communities in well-mixed lacustrine environments like the Great Lakes. Future work should
322 aim to sample a diverse range of environments to explore this possibility. The data from Lake
323 Erie suggest, however, that changes in ϵ_{por} throughout the sediment record in the Great Lakes
324 can be used to indicate how (or if) the relative contribution of cyanobacteria to primary
325 production shifted under pre-anthropogenic conditions in response to climate patterns and
326 nutrient supply and assist in differentiating between natural and anthropogenic influences on
327 phytoplankton community dynamics.

328

329 **5. Conclusions**

330 This study demonstrates that the chlorophyll ^{15}N fractionation patterns observed in
331 laboratory cultures are also observed in a natural phytoplankton community. ϵ_{por} values can
332 therefore be used to quantify the relative importance of cyanobacteria and eukaryotic algae in
333 past and present lacustrine environments. Future work should aim to elucidate the biosynthetic or
334 physiological mechanism that underlies these characteristic N isotope patterns among major
335 algal groups, as understanding how phytoplankton differ in their acquisition and intracellular
336 partitioning of N may have both evolutionary and biogeochemical implications.

337

338 **Acknowledgements**

339 The authors thank CIGLR and the NOAA Great Lakes Environmental Research
340 Laboratory (NOAA-GLERL) for allowing us to participate in their weekly HABs monitoring
341 program, Mr. Duane Gossiaux, Mr. Dack Stuart and Mrs. Christine Kitchens for field support,
342 and NOAA-GLERL captains and crew for logistical support. We also thank the Cooperative
343 Institute of Great Lakes Research (CIGLR) for nutrient data. The manuscript benefitted from

344 comments by Dr Yeuhan Lu and an anonymous reviewer, and we thank Dr Philip Meyers for
345 editorial handling. Funding was provided by the Gordon and Betty Moore Foundation, and by
346 NASA-Exobiology NNX16AJ52G (to A.P.). This is GLERL Publication No. XXXXX.

347

348 *Associate Editor*–**Philip A. Meyers**

349

350 **References**

- 351 Allinger, L., Reavie, E., 2013. The ecological history of Lake Erie as recorded by the
352 phytoplankton community. *Journal of Great Lakes Research* 39, 365–382.
- 353 Beale, S.I., 1999. Enzymes of chlorophyll biosynthesis. *Photosynthesis Research* 60, 43–73.
- 354 Beaumont, V., Jahnke, L., Des Marais, D., 2000. Nitrogen isotopic fractionation in the synthesis
355 of photosynthetic pigments in *Rhodobacter capsulatus* and *Anabaena cylindrica*. *Organic*
356 *Geochemistry* 31, 1075–1085.
- 357 Berry, M.A., Davis, T.W., Cory, R.M., Duhaime, M.B., Johengen, T.H., Kling, G.W., Marino,
358 J.A., Den Uyl, P.A., Gossiaux, D., Dick, G.J., Deneff, V.J., 2017. Cyanobacterial harmful
359 algal blooms are a biological disturbance to Western Lake Erie bacterial communities.
360 *Environmental Microbiology* 19, 1149–1162.
- 361 Beutler, M., Wiltshire, K., Meyer, B., Moldaenke, C., Lüring, C., Meyerhöfer, M., Hansen, U.P.,
362 Dau, H., 2002. A fluorometric method for the differentiation of algal populations *in vivo*
363 and *in situ*. *Photosynthesis Research* 72, 39–53.
- 364 Bridgeman, T.B., Chaffin, J.D., Kane, D.D., Conroy, J.D., Panek, S.E., Armenio, P.M., 2012.
365 From River to Lake: Phosphorus partitioning and algal community compositional changes
366 in Western Lake Erie. *Journal of Great Lakes Research* 38, 90–97.

367 Calvert, S.E., Nielsen, B., Fontugne, M.R., 1992. Evidence from nitrogen isotope ratios for
368 enhanced productivity during formation of eastern Mediterranean sapropels. *Nature* 359,
369 223–225.

370 Carmichael, W., Boyer, G.L., 2016. Health impacts from cyanobacteria harmful algae blooms:
371 implications for the North American Great Lakes. *Harmful Algae* 54, 194–212.

372 Chicarelli, M.I., Hayes, J.M., Popp, B.N., Eckardt, C.B., Maxwell, J.R., 1993. Carbon and
373 nitrogen isotopic compositions of alkyl porphyrins from the Triassic Serpiano oil shale.
374 *Geochimica et Cosmochimica Acta* 57, 1307–1311.

375 Chikaraishi, Y., Kashiya, Y., Ogawa, N.O., Kitazato, H., Satoh, M., Nomoto, S., Ohkouchi,
376 N., 2008. A compound-specific isotope method for measuring the stable nitrogen isotopic
377 composition of tetrapyrroles. *Organic Geochemistry* 39, 510–520.

378 Del Giudice, D., Zhou, Y., Sinha, E., Michalak, A.M., 2018. Long-term phosphorus loading and
379 springtime temperatures explain interannual variability of hypoxia in a large temperate lake.
380 *Environmental Science & Technology* 52, 2046–2054.

381 Escoffier, N., Bernard, C., Hamlaoui, S., Groleau, A., Catherine, A., 2015. Quantifying
382 phytoplankton communities using spectral fluorescence : the effects of species composition
383 and physiological state. *Journal of Plankton Research* 37, 233–247.

384 Fulton, J.M., Arthur, M.A., Freeman, K.H., 2012. Black Sea nitrogen cycling and the
385 preservation of phytoplankton $\delta^{15}\text{N}$ signals during the Holocene. *Global Biogeochemical*
386 *Cycles* 26, 1–15.

387 Fulton, J.M., Arthur, M.A., Thomas, B., Freeman, K.H., 2018. Pigment carbon and nitrogen
388 isotopic signatures in euxinic basins. *Geobiology* 16, 429–445.

389 Glibert, P.M., Fullerton, D., Burkholder, J.M., Cornwel, J.C., Kana, T.M., 2011. Ecological

390 stoichiometry, biogeochemical bycling, invasive species, and aquatic food webs: San
391 Francisco Estuary and comparative systems. *Reviews in Fisheries Science* 19, 358–417.

392 Godfrey, L.V., Falkowski, P.G., 2009. The cycling and redox state of nitrogen in the Archaean
393 ocean. *Nature Geoscience* 2, 725–729.

394 Gueneli, N., McKenna, A.M., Ohkouchi, N., Boreham, C.J., Beghin, J., Javaux, E.J., Brocks, J.J.,
395 2018. 1.1-Billion-year-old porphyrins establish a marine ecosystem dominated by bacterial
396 primary producers. *Proceedings of the National Academy of Sciences* 115, E6978–E6986.

397 Hayes, J.M., 2001. Fractionation of carbon and hydrogen isotopes in biosynthetic processes.
398 *Reviews in Mineralogy and Geochemistry* 43, 225–277.

399 Higgins, M.B., Robinson, R.S., Casciotti, K.L., McIlvin, M.R., Pearson, A., 2009. A method for
400 determining the nitrogen isotopic composition of porphyrins. *Analytical Chemistry* 81, 184–
401 192.

402 Higgins, M.B., Robinson, R.S., Husson, J.M., Carter, S.J., Pearson, A., 2012. Dominant
403 eukaryotic export production during ocean anoxic events reflects the importance of recycled
404 NH_4^+ . *Proceedings of the National Academy of Sciences* 109, 2269–2274.

405 Higgins, M.B., Wolfe-Simon, F., Robinson, R.S., Qin, Y., Saito, M.A., Pearson, A., 2011.
406 Paleoenvironmental implications of taxonomic variation among ^{15}N values of
407 chloropigments. *Geochimica et Cosmochimica Acta* 75, 7351–7363.

408 Hobbs, W.O., Lafrancois, B.M., Stottlemyer, R., Toczydlowski, D., Engstrom, D.R., Edlund,
409 M.B., Almendinger, J.E., Strock, K.E., VanderMeulen, D., Elias, J.E., Saros, J.E., 2016.
410 Nitrogen deposition to lakes in national parks of the western Great Lakes region: Isotopic
411 signatures, watershed retention, and algal shifts. *Global Biogeochemical Cycles* 514–533.

412 Hodell, D.A., Schelske, C.L., 1998. Production, sedimentation, and isotopic composition of

413 organic matter in Lake Ontario. *Limnology and Oceanography* 43, 200–214.

414 Ishikawa, N.F., Yamane, M., Suga, H., Ogawa, N.O., Yokoyama, Y., Ohkouchi, N., 2015.

415 Chlorophyll *a*-specific $\Delta^{14}\text{C}$, $\delta^{13}\text{C}$ and $\delta^{15}\text{N}$ values in stream periphyton: Implications for

416 aquatic food web studies. *Biogeosciences* 12, 6781–6789.

417 Jenkyns, H.C., Gröcke, D.R., Hesselbo, S.P., 2001. Nitrogen isotope evidence for water mass

418 denitrification during the early Toarcian (Jurassic) oceanic anoxic event. *Paleoceanography*

419 16, 593–603.

420 Johnsen, G., Sakshaug, E., 2007. Biooptical characteristics of PSII and PSI in 33 species (13

421 pigment groups) of marine phytoplankton, and the relevance for pulse-amplitude-modulated

422 and fast-repetition-rate fluorometry. *Journal of Phycology* 43, 1236–1251.

423 Junium, C.K., Freeman, K.H., Arthur, M.A., 2015. Controls on the stratigraphic distribution and

424 nitrogen isotopic composition of zinc, vanadyl and free base porphyrins through Oceanic

425 Anoxic Event 2 at Demerara Rise. *Organic Geochemistry* 80, 60–71.

426 Katase, T., Wada, E., 1990. Isolation of chlorophyll *a* in *Microcystis* spp. for determination of

427 stable isotopes of carbon and nitrogen, and variation in Suwa lake, Japan. *Japan Anal.* 39,

428 451–456.

429 Leavitt, P.R., 1993. A review of factors that regulate carotenoid and chlorophyll deposition and

430 fossil pigment abundance. *Journal of Paleolimnology* 9, 109–127.

431 Leavitt, P.R., Findlay, D.L., 1994. Comparison of fossil pigments with 20 years of phytoplankton

432 data from eutrophic Lake 227, Experimental Lakes Area, Ontario. *Canadian Journal of*

433 *Fisheries and Aquatic Sciences* 51, 2286–2299.

434 Louda, J.W., Baker, E.W., 1986. The biogeochemistry of chlorophyll. In: Sohn, H.L. (Ed.),

435 *Organic Marine Geochemistry*. American Chemical Society, Washington, DC, pp. 107–126.

436 Michalak, A.M., Anderson, E.J., Beletsky, D., Boland, S., Bosch, N.S., Bridgeman, T.B.,
437 Chaffin, J.D., Cho, K., Confesor, R., Daloglu, I., DePinto, J. V., Evans, M.A., Fahnenstiel,
438 G.L., He, L., Ho, J.C., Jenkins, L., Johengen, T.H., Kuo, K.C., LaPorte, E., Liu, X.,
439 McWilliams, M.R., Moore, M.R., Posselt, D.J., Richards, R.P., Scavia, D., Steiner, A.L.,
440 Verhamme, E., Wright, D.M., Zagorski, M.A., 2013. Record-setting algal bloom in Lake
441 Erie caused by agricultural and meteorological trends consistent with expected future
442 conditions. *Proceedings of the National Academy of Sciences* 110, 6448–6452.

443 Ren, H., Sigman, D.M., Meckler, A.N., Plessen, B., Robinson, R.S., Rosenthal, Y., Haug, G.H.,
444 2009. Foraminiferal isotope evidence of reduced nitrogen fixation in the ice age Atlantic
445 ocean. *Science* 323, 244–248.

446 Robinson, R.S., Brunelle, B.G., Sigman, D.M., 2004. Revisiting nutrient utilization in the glacial
447 Antarctic: Evidence from a new method for diatom-bound N isotopic analysis.
448 *Paleoceanography* 19. doi:10.1029/2003PA000996

449 Robinson, R.S., Kienast, M., Luiza Albuquerque, A., Altabet, M., Contreras, S., De Pol Holz, R.,
450 Dubois, N., Francois, R., Galbraith, E., Hsu, T.C., Ivanochko, T., Jaccard, S., Kao, S.J.,
451 Kiefer, T., Kienast, S., Lehmann, M., Martinez, P., McCarthy, M., Möbius, J., Pedersen, T.,
452 Quan, T.M., Ryabenko, E., Schmittner, A., Schneider, R., Schneider-Mor, A., Shigemitsu,
453 M., Sinclair, D., Somes, C., Studer, A., Thunell, R., Yang, J.Y., 2012. A review of nitrogen
454 isotopic alteration in marine sediments. *Paleoceanography* 27. doi:10.1029/2012PA002321

455 Sachs, J.P., Repeta, D.J., Goericke, R., 1999. Nitrogen and carbon isotopic ratios of chlorophyll
456 from marine phytoplankton. *Geochimica et Cosmochimica Acta* 63, 1431–1441.

457 Shen, J., Pearson, A., Henkes, G.A., Zhang, Y.G., Chen, K., Li, D., Wankel, S.D., Finney, S.C.,
458 Shen, Y., 2018a. Improved efficiency of the biological pump as a trigger for the Late

459 Ordovician glaciation. *Nature Geoscience* 11, 510–514.

460 Sigman, D., Karsh, K., Casciotti, K., 2009. Ocean process tracers: nitrogen isotopes in the ocean,
461 in: *Encyclopedia of Ocean Sciences*. pp. 4138–4153.

462 Sigman, D.M., Altabet, M.A., Francois, R., McCorkle, D.C., Gaillard, J.-F., 1999. The isotopic
463 composition of diatom-bound nitrogen in Southern Ocean sediments. *Paleoceanography*
464 14, 118–134.

465 Sigman, D.M., Casciotti, K.L., Andreani, M., Barford, C., Galanter, M., Bhlke, J.K., Bo, J.K.,
466 Supe, Ä.N., 2001. A bacterial method for the nitrogen isotopic analysis of nitrate in
467 seawater and freshwater. *Analytical Chemistry* 73, 4145–4153.

468 Struck, U., Emeis, K.C., Voss, M., Christiansen, C., Kunzendorf, H., 2000. Records of southern
469 and central Baltic Sea eutrophication in $\delta^{13}\text{C}$ and $\delta^{15}\text{N}$ of sedimentary organic matter.
470 *Marine Geology* 164, 157–171.

471 Stumpf, R.P., Wynne, T.T., Baker, D.B., Fahnenstiel, G.L., 2012. Interannual variability of
472 cyanobacterial blooms in Lake Erie. *PLoS ONE* 7. doi:10.1371/journal.pone.0042444

473 Taranu, Z.E., Gregory-Eaves, I., Leavitt, P.R., Bunting, L., Buchaca, T., Catalan, J., Domaizon,
474 I., Guilizzoni, P., Lami, A., McGowan, S., Moorhouse, H., Morabito, G., Pick, F.R.,
475 Stevenson, M.A., Thompson, P.L., Vinebrooke, R.D., 2015. Acceleration of cyanobacterial
476 dominance in north temperate-subarctic lakes during the Anthropocene. *Ecology Letters* 18,
477 375–384.

478 Teranes, J.L., Bernasconi, S.M., 2000. The record of nitrate utilization and productivity
479 limitation provided by $\delta^{15}\text{N}$ values in lake organic matter – a study of sediment trap and
480 core sediments from Baldeggersee, Switzerland. *Limnology and Oceanography* 45, 801–
481 813.

482 Tesdal, J.-E., Galbraith, E.D., Kienast, M., 2013. Nitrogen isotopes in bulk marine sediment:
483 Linking seafloor observations with subseafloor records. *Biogeosciences* 10, 101–118.

484 Tsao, L.E., Robinson, R.S., Higgins, M.B., Pearson, A., 2012. Nitrogen isotope ratio of
485 cyanobacterial chlorophyll: Chemostat vs. batch culture. *Organic Geochemistry* 49, 96–99.

486 Tyler, J., Kashiyama, Y., Ohkouchi, N., Ogawa, N.O., Yokoyama, Y., Chikaraishi, Y., Staff,
487 R.A., Ikehara, M., Bronk Ramsey, C., Bryant, C., Brock, F., Gotanda, K., Haraguchi, T.,
488 Yonenobu, H., Nakagawa, T., 2010. Tracking aquatic change using chlorine-specific carbon
489 and nitrogen isotopes: The last glacial-interglacial transition at Lake Suigetsu, Japan.
490 *Geochemistry Geophysics Geosystems* 11. doi:10.1029/2010gc003186

491 Zhou, Y., Obenour, D.R., Scavia, D., Johengen, T.H., Michalak, A.M., 2013. Spatial and
492 temporal trends in Lake Erie hypoxia, 1987 – 2007. *Environmental Science and Technology*
493 47, 899–905.

494

495 **Figure Captions**

496

497 **Fig. 1.** Summary of ϵ_{por} values ($\epsilon_{\text{por}} = \delta^{15}\text{N}_{\text{biomass}} - \delta^{15}\text{N}_{\text{chloropigment}}$) obtained from previous studies
498 of pure cultures (Sachs et al., 1999; Beaumont et al., 2000; Higgins et al., 2011; Tsao et al.,
499 2012), where n = number of experiments. In each box, the black circle indicates the average, the
500 central line indicates the median, and the bottom and top edges of the box indicate the 25th and
501 75th percentiles, respectively. The whiskers extend to the most extreme data points.

502

503 **Fig. 2.** Map of GLERL master stations in western Lake Erie, highlighting the location of station
504 WE2. Inset is a satellite image of Lake Erie in late July 2017 showing the location of the CHAB
505 in the western basin (photo credit: NOAA GLERL).

506

507 **Fig. 3.** Community composition as measured by Fluoroprobe (A), $\delta^{15}\text{N}$ values of chlorophyll and
508 bulk particulate organic matter (B), and calculated ϵ_{por} values (C) over the summer. For ease of
509 viewing error bars are not shown in (A), but uncertainty in Fluoroprobe measurements is
510 estimated at $\pm 5\%$. In (B) and (C), if not visible, error bars are smaller than the size of the
511 symbols.

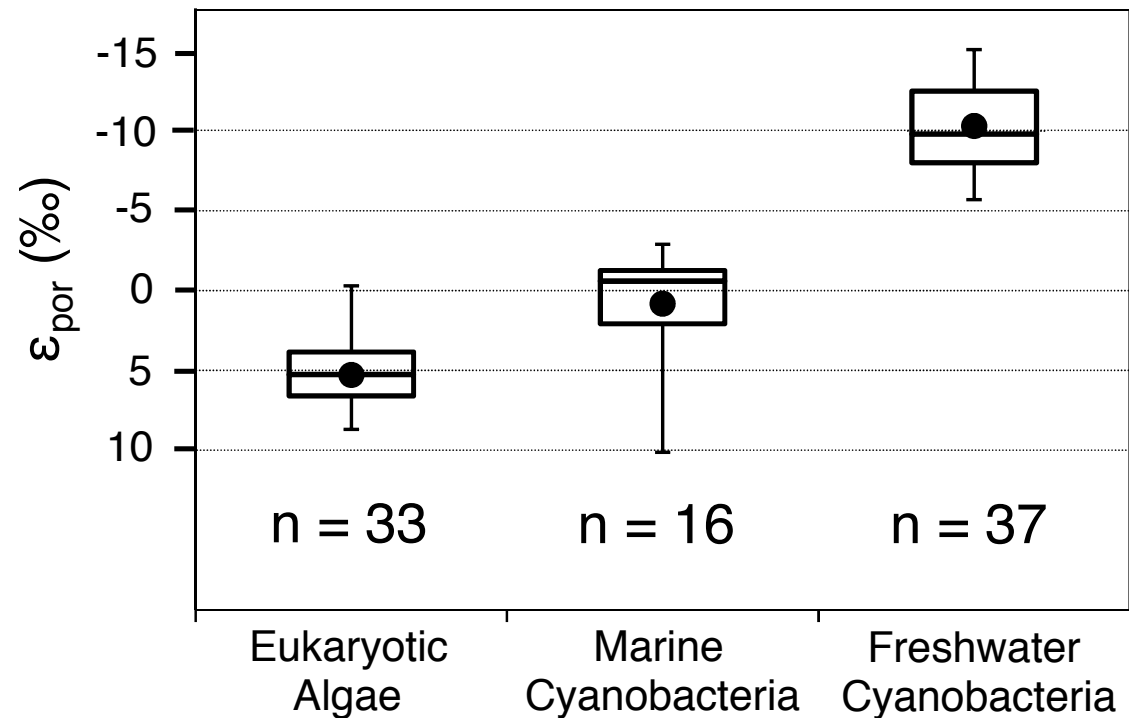
512

513 **Fig. 4.** The correlation between Lake Erie ϵ_{por} values (blue diamonds) and the fraction of the
514 community consisting of cyanobacteria. Data are fit with an ordinary linear least-squares
515 regression (black line) and an orthogonal (Deming) least-squares regression (red line). The green
516 shaded region indicates the median and standard deviation of ϵ_{por} from eukaryotic lab cultures
517 ($5.5 \pm 1.6\%$), while the orange shaded region indicates the same from cyanobacterial lab cultures
518 ($-10.3 \pm 1.8\%$). The orange diamond indicates the most extreme ϵ_{por} value observed to date in
519 lab cultures of cyanobacteria (-14.1%), while the purple diamond indicates the ϵ_{por} value of
520 -16% observed in a freshwater lake dominated by cyanobacteria (Katase and Wada, 1990).

521

522

523



Western Lake Erie Master Stations



WE8

WE4



WE2

WE13

WE6

WE12

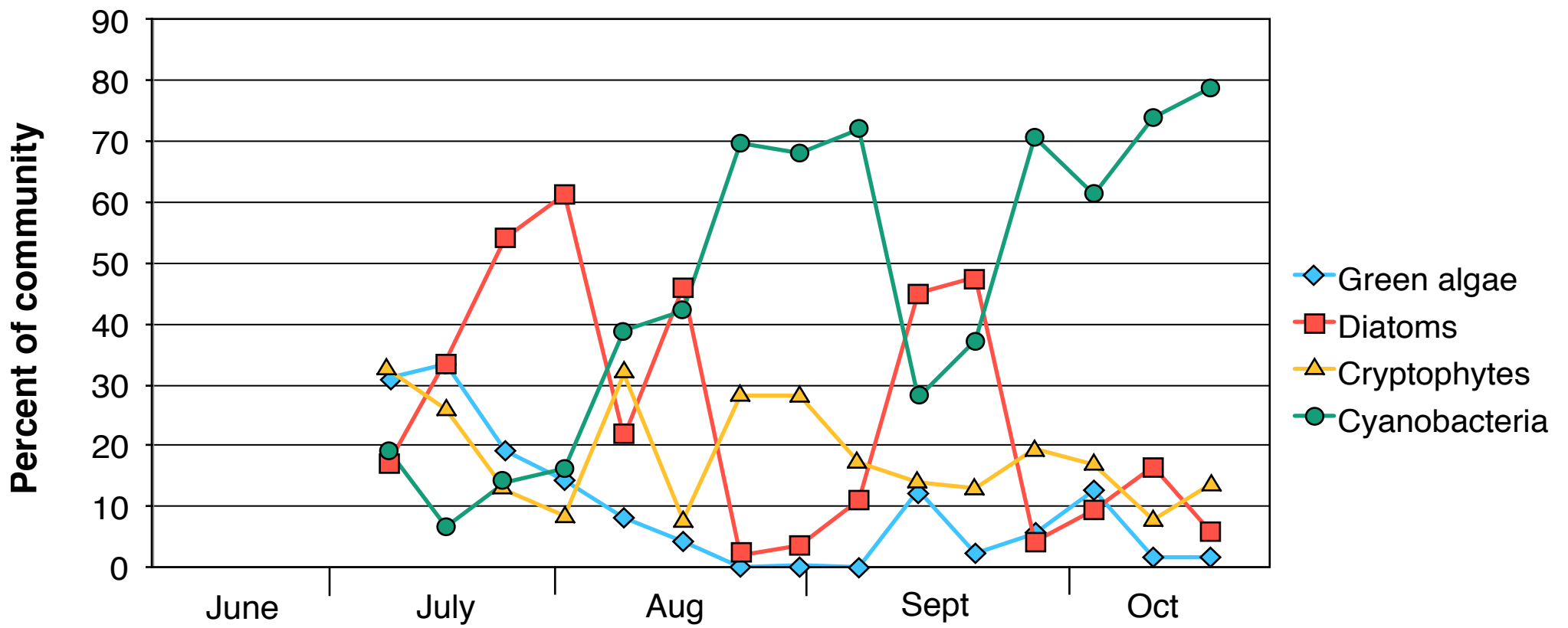
WE14

WE15

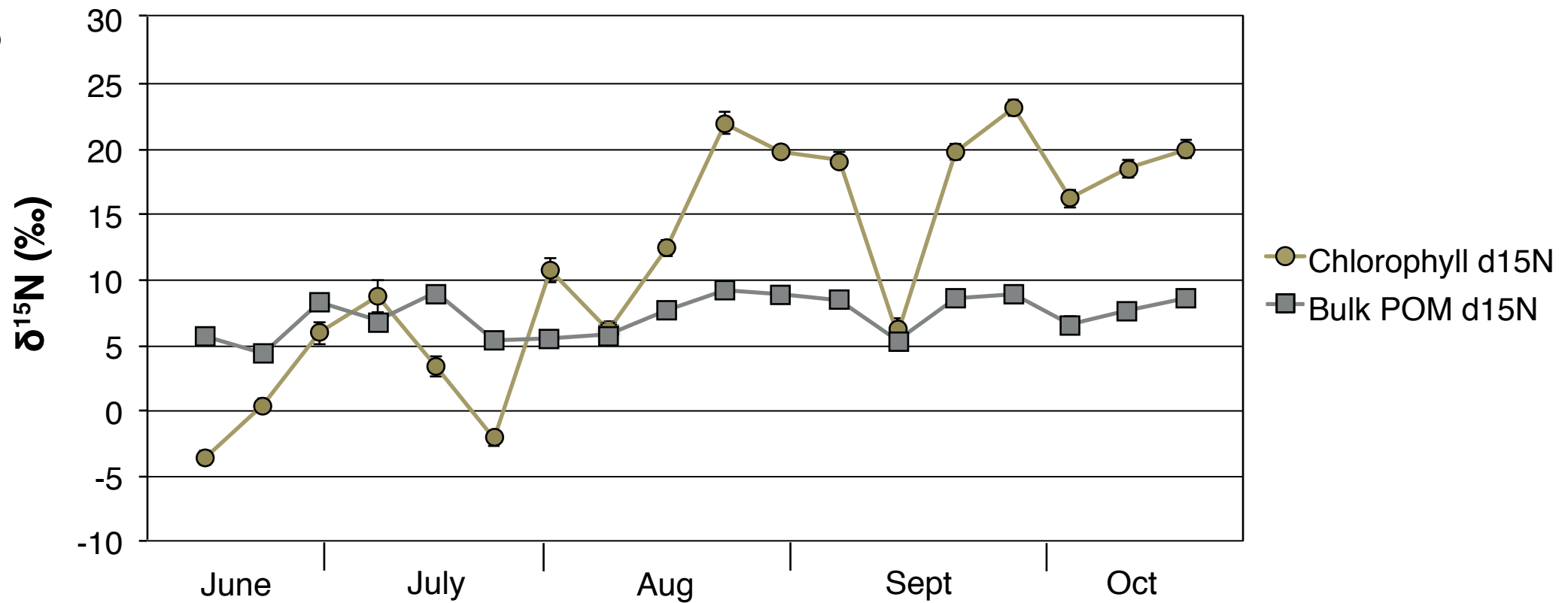


0 5 10km

A



B



C

